5th Sino–German symposium “The silicon age“
杭州 2015-09

Thermoelectricity of silicon nanostructures

Hartmut S. Leipner

Katrin Bertram, Markus Trutschel, Bodo Fuhrmann,

Aleksander Tonkikh*, Peter Werner*

Martin-Luther-Universität Halle–Wittenberg

*Max-Planck-Institut für Mikrostrukturphysik Halle

Martin-Luther-Universität Halle–Wittenberg

Weinberg Campus

Interdisciplinary Center of Materials Science

Nanotechnology pilot plant

- **Nanostructuring**: lithography, thin film deposition, device prototyping
- **Nanoanalysis**: electron microscopy, optical spectroscopy, positron annihilation
- 1800 m^2 labs, 620 m^2 cleanroom

Research

- **Energy conversion:** photovoltaics, photonics
- **Energy storage:** batteries
- **Energy recycling:** thermoelectrics

Thermoelectric devices

Thermoelectric generator

- Heat → electricity
- Heat flow drives free e⁻ and h⁺ from hot to cold

Seebeck effect

$$U = \int_{T_1}^{T_2} S \, \mathrm{d}T$$

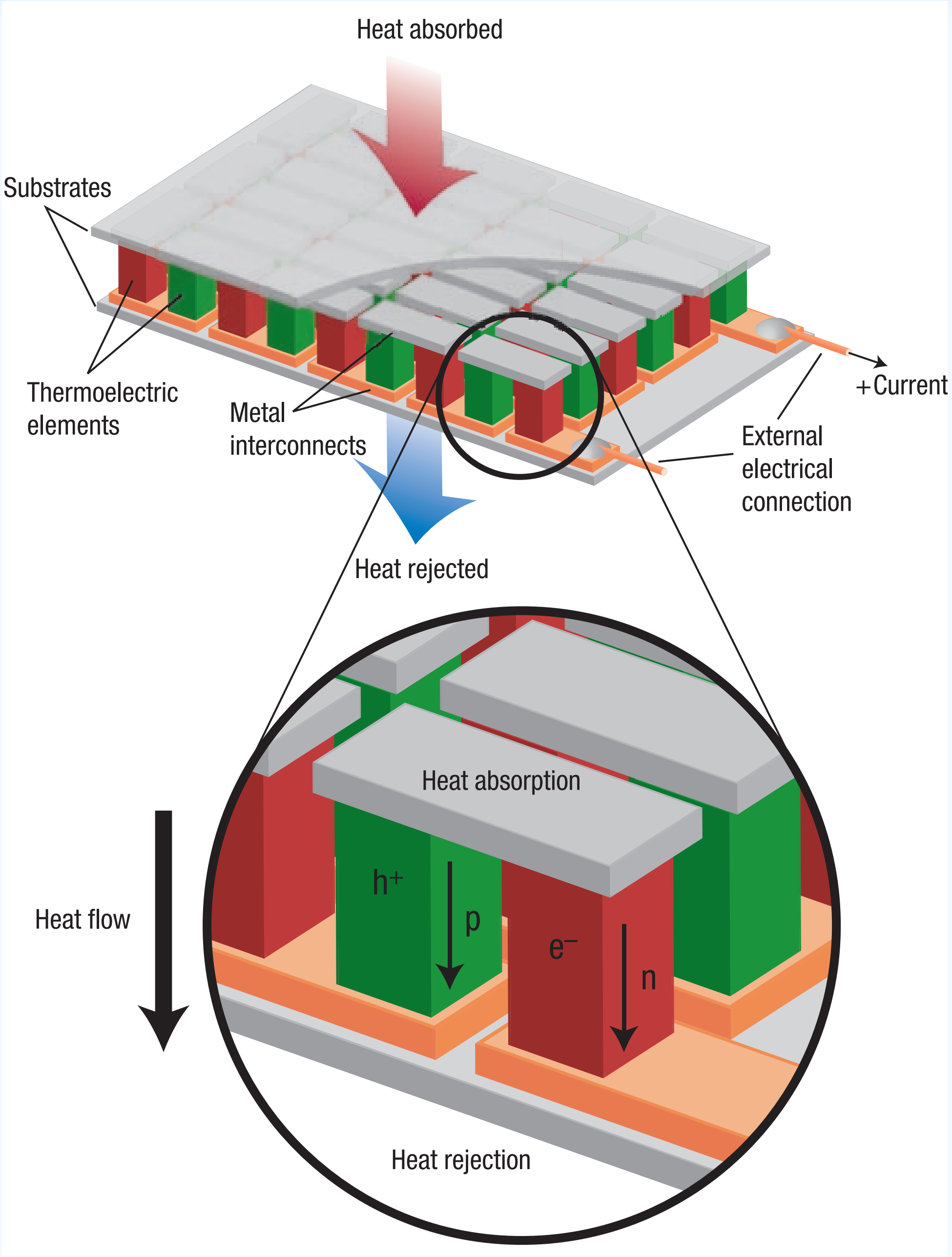

[Snyder, Toberer 2008]

Thermoelectrics

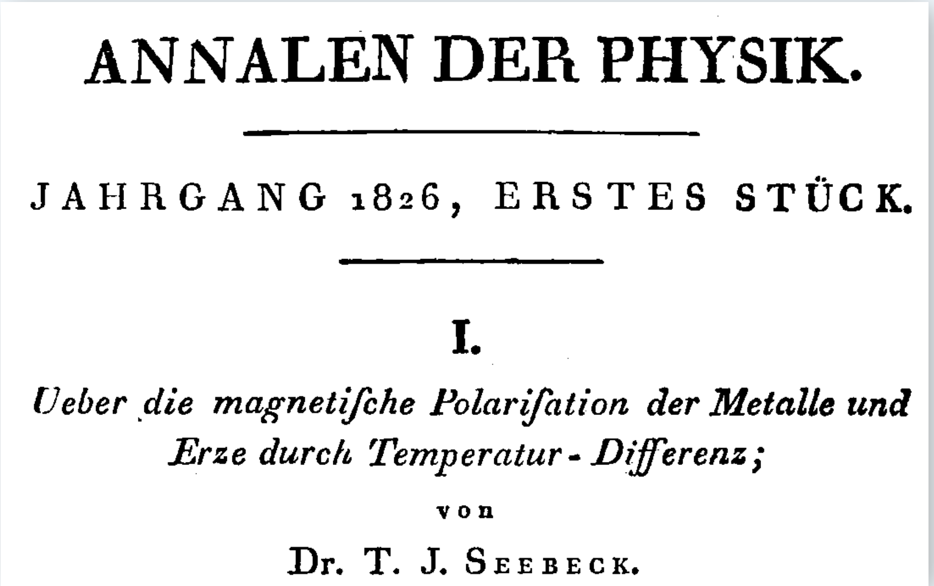
ANNALEN DER PHYSIK.

JAHRGANG 1826, ERSTES STÜCK.

I.

Ueber die magnetiſche Polariſation der Metalle und Erze durch Temperatur-Differenz;

von

Dr. T. J. Seebeck.

Thomas J. Seebeck
(1770–1831)

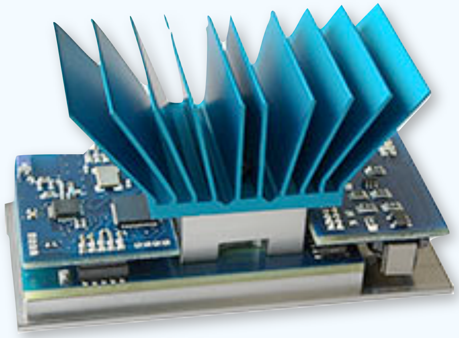

Power Node
[Micropelt]

[NASA]

Basic terms of thermoelectrics

Conversion efficiency

- Determined by the dimensionless figure of merit

$$ZT = \frac{S^2\sigma}{\kappa}T$$

($S^2\sigma$ power factor, σ electrical conductivity, κ thermal conductivity, T temperature)

- High ZT requires $S^2\sigma \uparrow$ and $\kappa = \kappa_e + \kappa_{ph} \downarrow$
- Problem: Coupling between electrical and thermal conductivity
- Topical materials $ZT \leq 1$
- Taylor materials by nanostructuring: Superlattices, nanowires, quantum dots

$\kappa \downarrow$	$S^2\sigma \uparrow$
Phonon glass	Electron crystal

Si as thermoelectric material

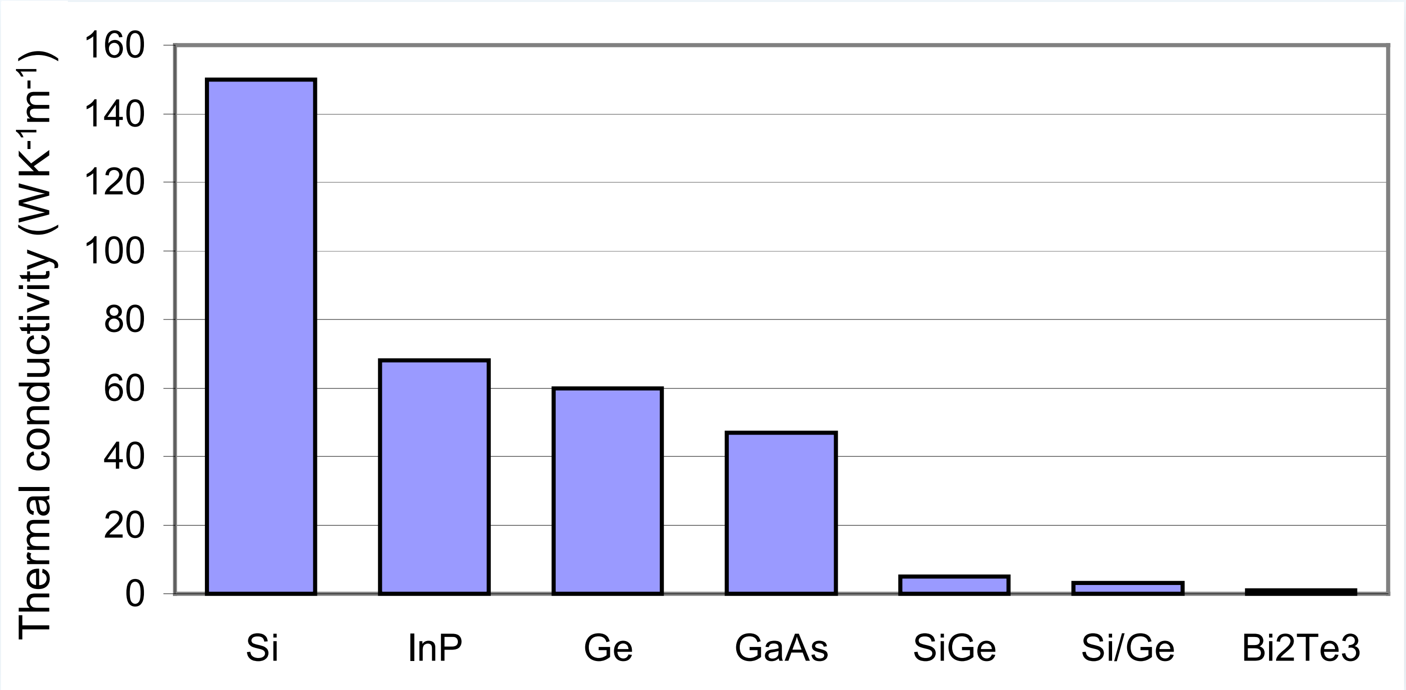

Thermal conductivity of the lattice κ_{ph} for semiconductor single crystals

[Fan 2002]

Nanostructuring

- Bandstructure engineering
- Phonon scattering at interfaces, porous surfaces, defects

Superlattices

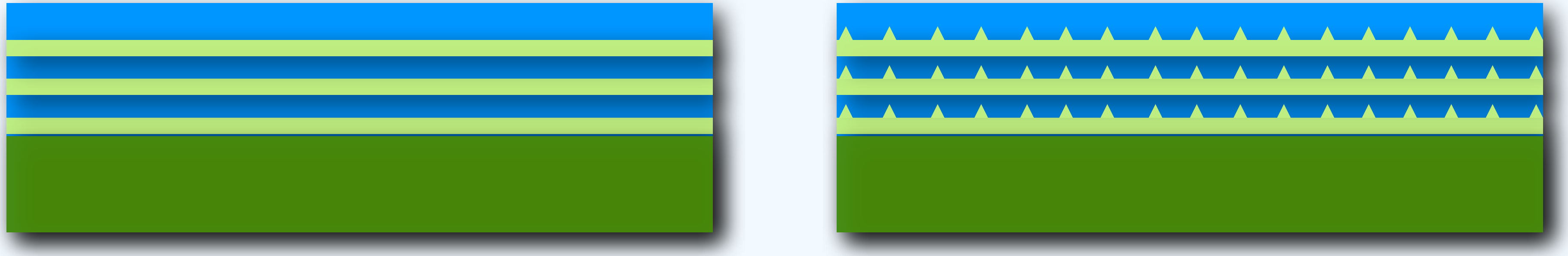

Single-crystalline multilayer and quantum dot superlattices

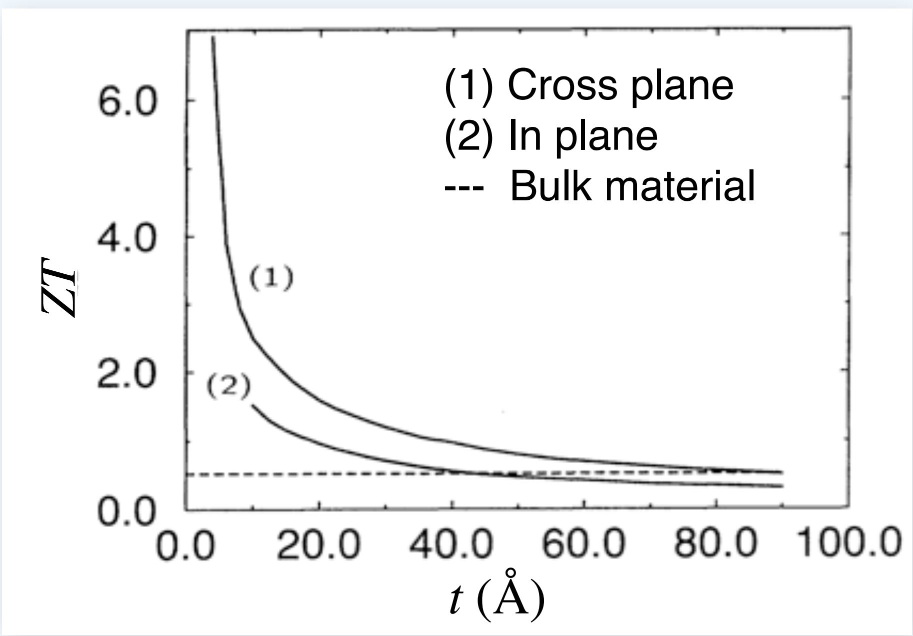

$$ZT = \frac{S^2\sigma}{\kappa_{\mathrm{ph}} + \kappa_{\mathrm{e}}} T$$

Thermoelectric efficiency ZT for anisotropic Bi_2Te_3 layers of the thickness t

[Hicks, Dresselhaus 1993]

Reduction of thermal conductivity

Cross-plane transport in SL → Coherent phonon scattering at interfaces

	Mean free path
Phonon	$\ell \approx 260$ nm
Electron	$\ell_e \sim 10$ nm

$$\kappa_{\text{ph}} = \frac{1}{3} C \upsilon \ell$$

(C lattice heat capacity, υ speed of sound)

If layer thickness $a < \ell$, the thermal conductivity of the lattice κ_{ph} is reduced.

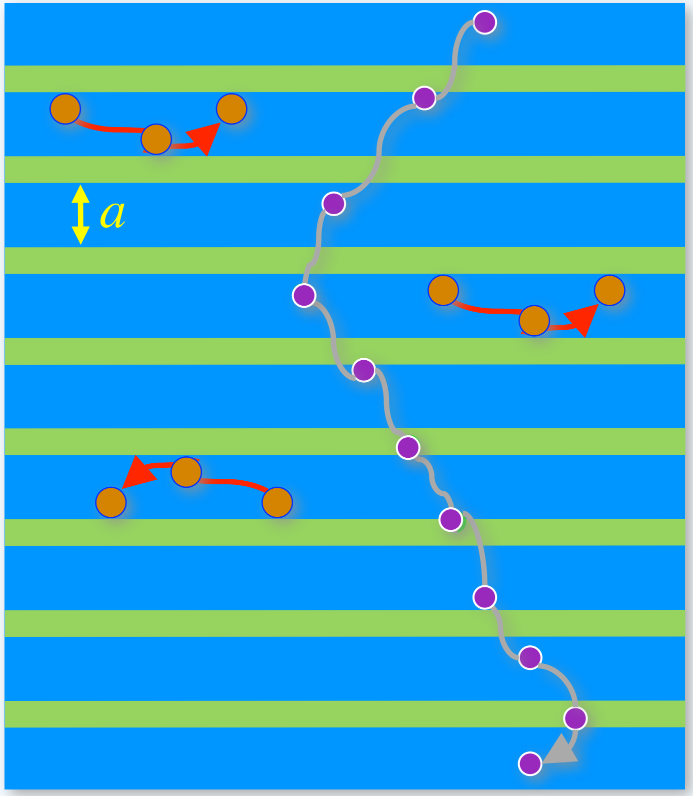

Phonon scattering at interfaces

Phonon scattering

Superlattices, composites, quantum dot SLs, random multilayers

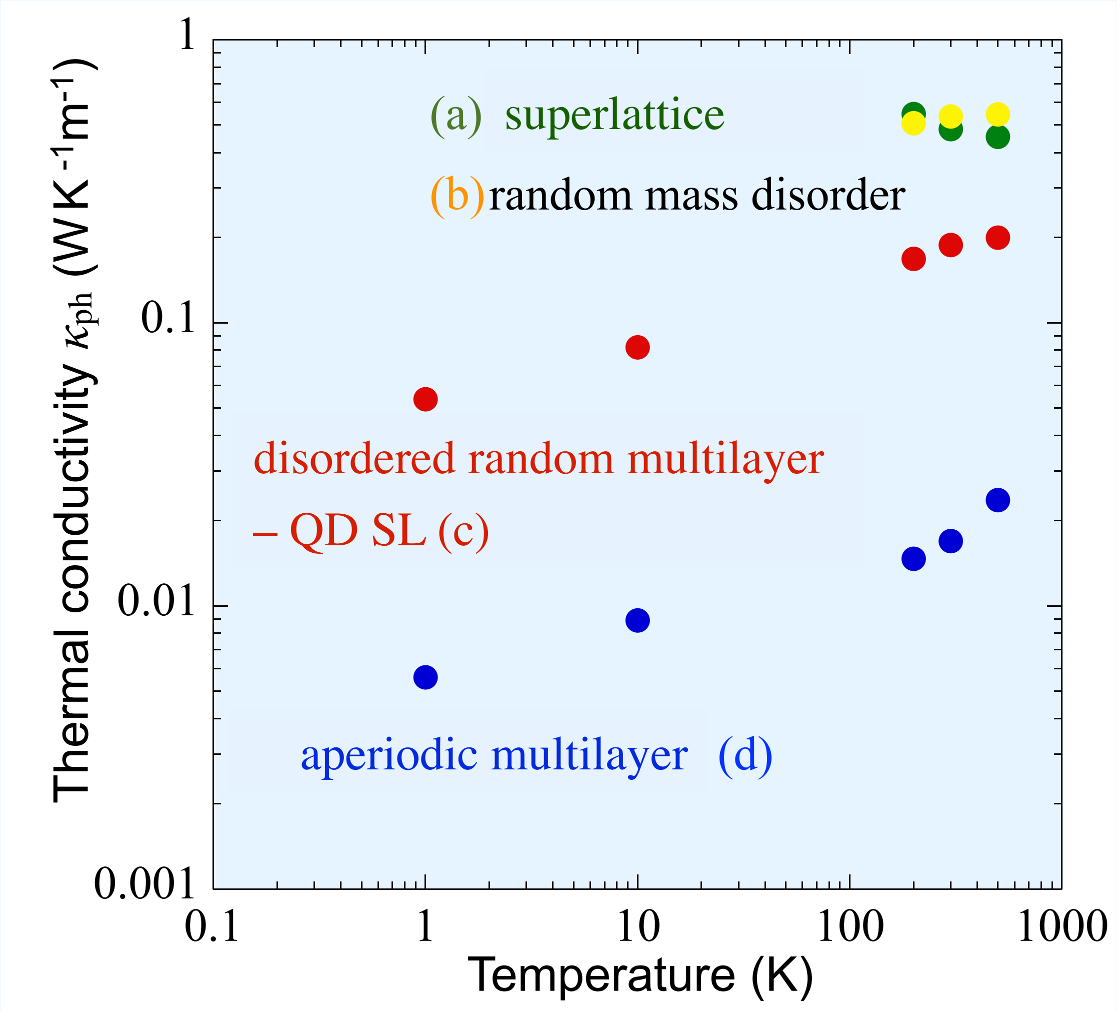

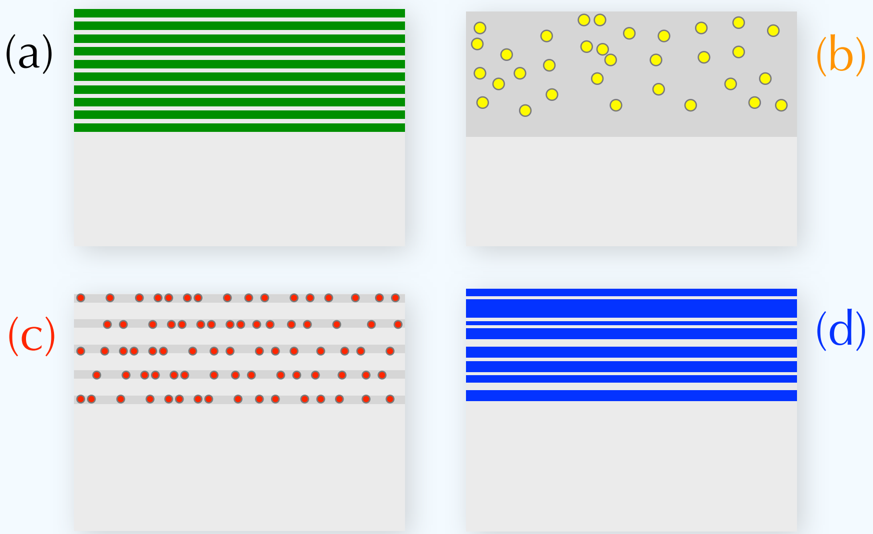

Anderson localization of phonons in **nonperiodic structures**

MD Simulation

[Frachioni, White 2012]

Reduction in the thermal conductivity

- Different approaches through nanostructures like
  - Superlattices (SL)
  - Nanowires (NW)
  - Quantum-dot superlattices (QDSL)
  - Nanowires containing superlattices (SLNW)

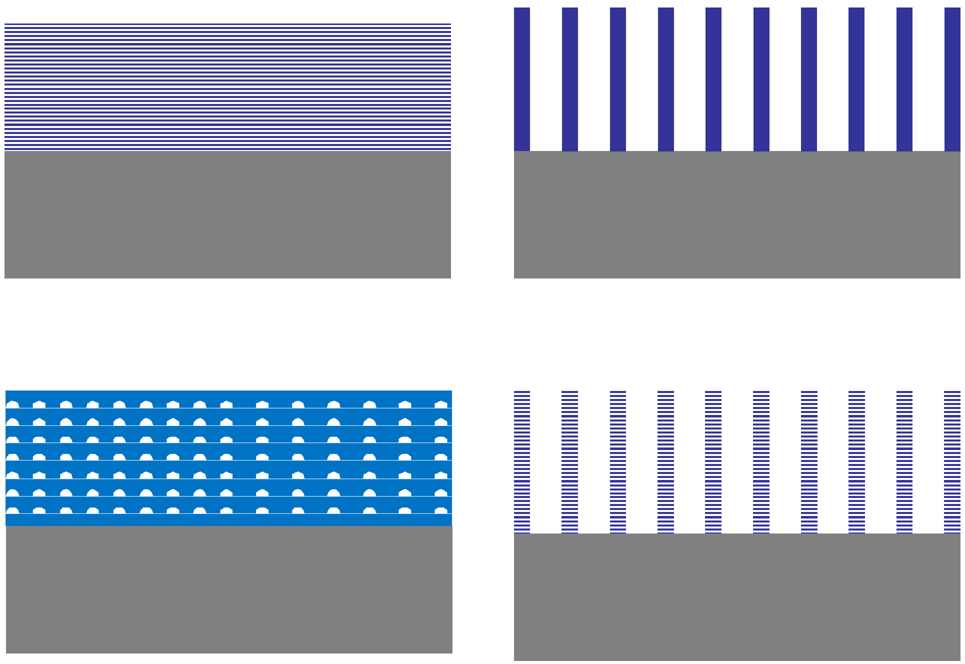

MBE of Si–Ge layers

- Stack of alternating layers of Si and $Si_{1-x}Ge_x$ alloy
- Precision of single layers: ± 0.2 nm

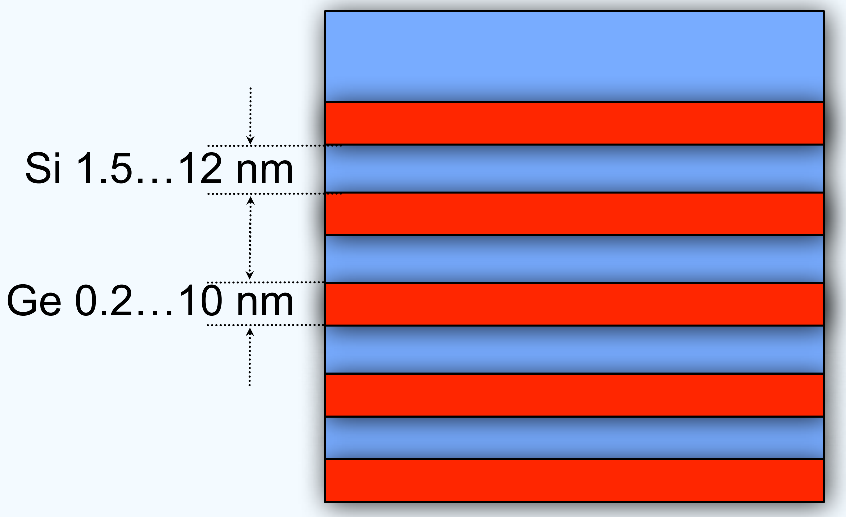

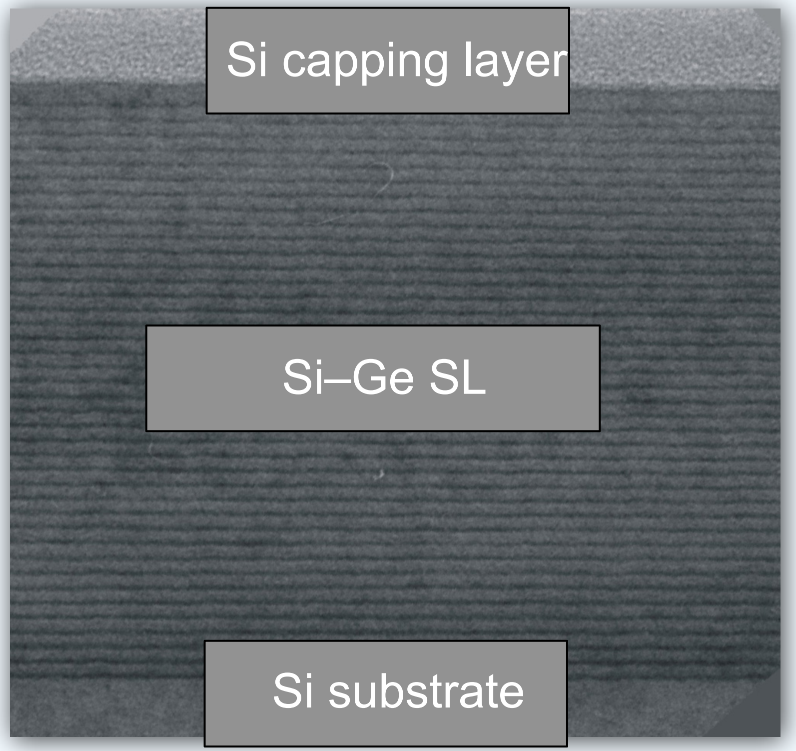

Quantum dot Si–Ge superlattice

- (001), (111) orientation of the Si substrate
- Si (111) → flat layers
- Si (100) → Ge islands (density ~ $10^9 \dots 10^{11}$ cm^{-2})

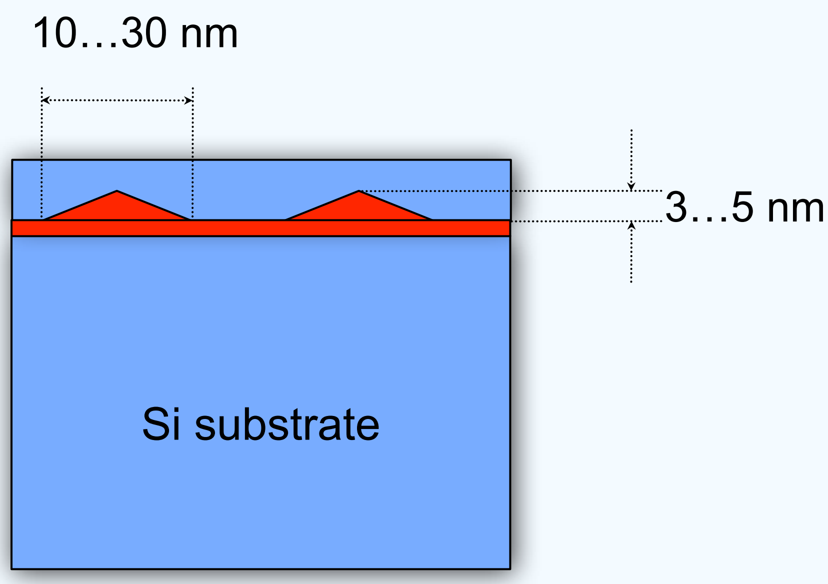

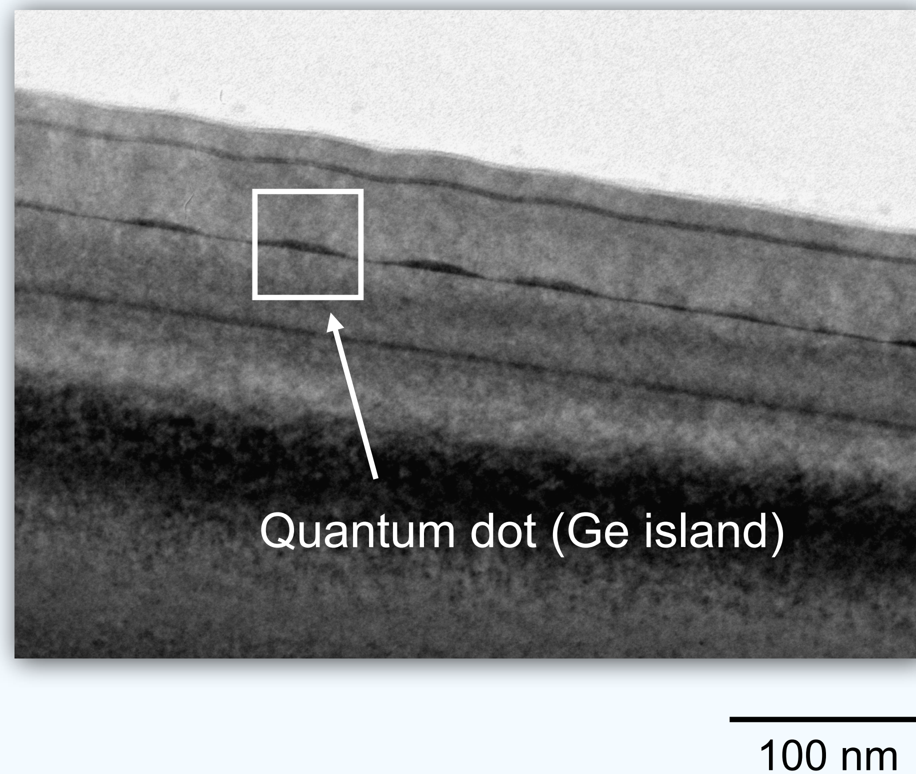

[Tonkikh *et al* 2011]

Cross-plane measurement

- Direct measurement of thin layers on a substrate rather demanding
- Cross-plane and in-plane electrical conductivity of specially designed samples (mesa) obtained via transmission line model
- Determination of the contact resistances
- Small error of resistivity measurement only with slight doping

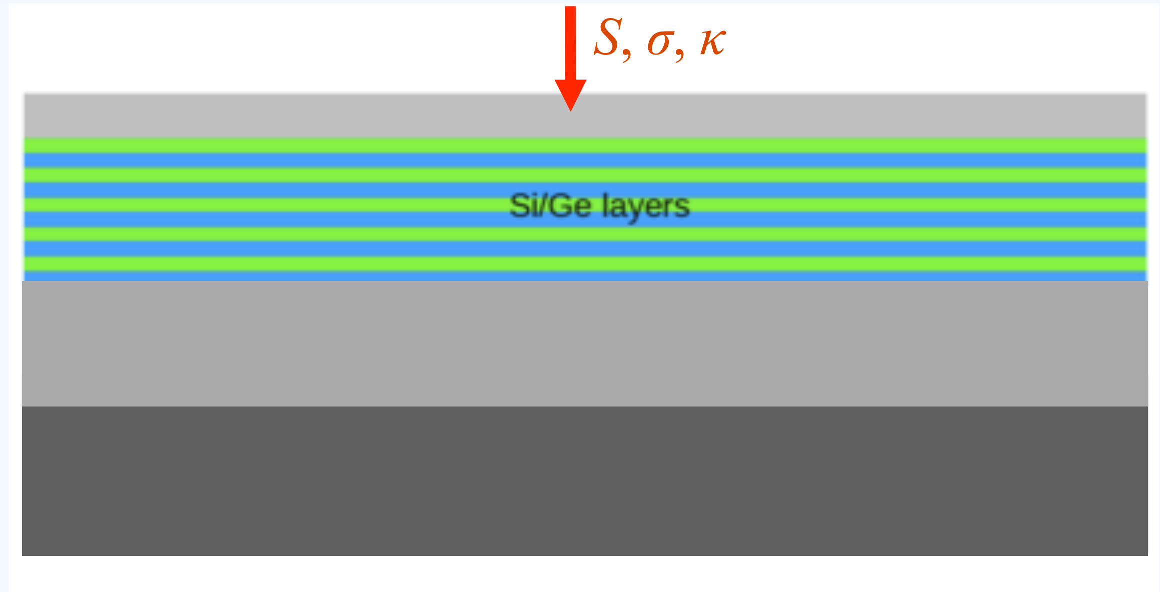

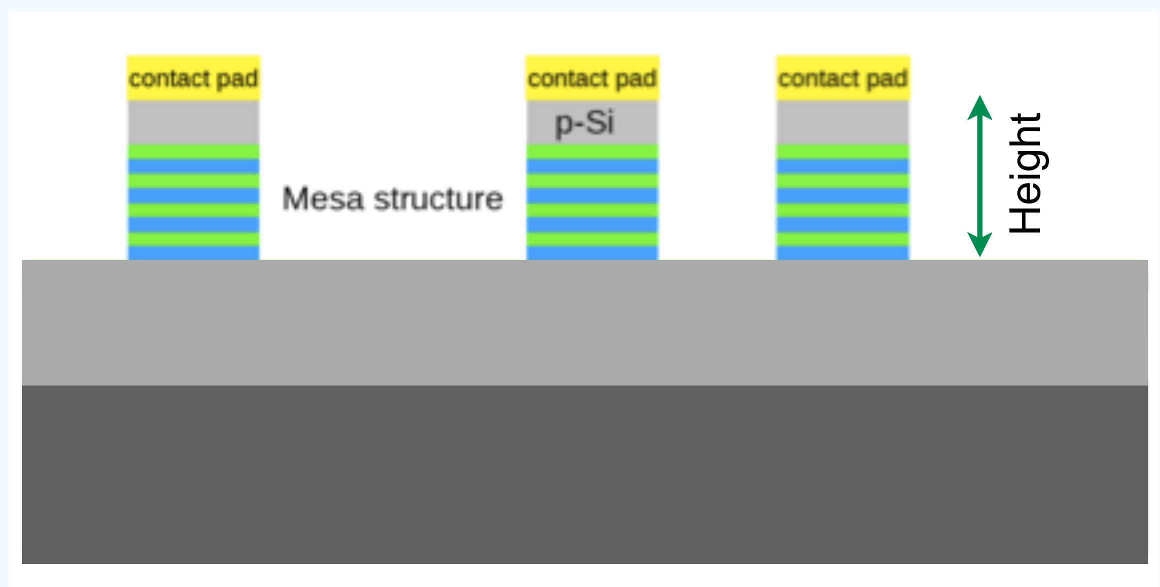

Current–voltage distribution

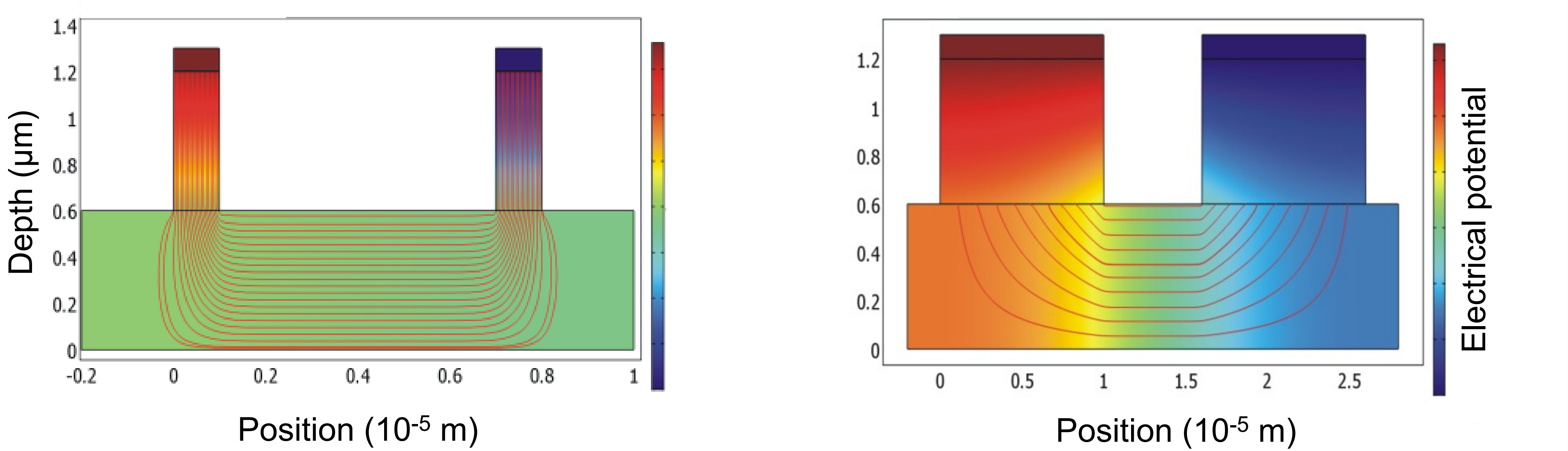

Finite-element simulation of the current–voltage distribution
in mesa structures of different widths

Seebeck cross-plane measurement

- Measurement of the thermoelectric voltage close to the superlattice mesa
- Metals 1 and 2 form the thermocouple
  → determination of the temperature difference ΔT
- Measurement of further thermovoltages to eliminate the in-plane contribution
- Where to place the heater?

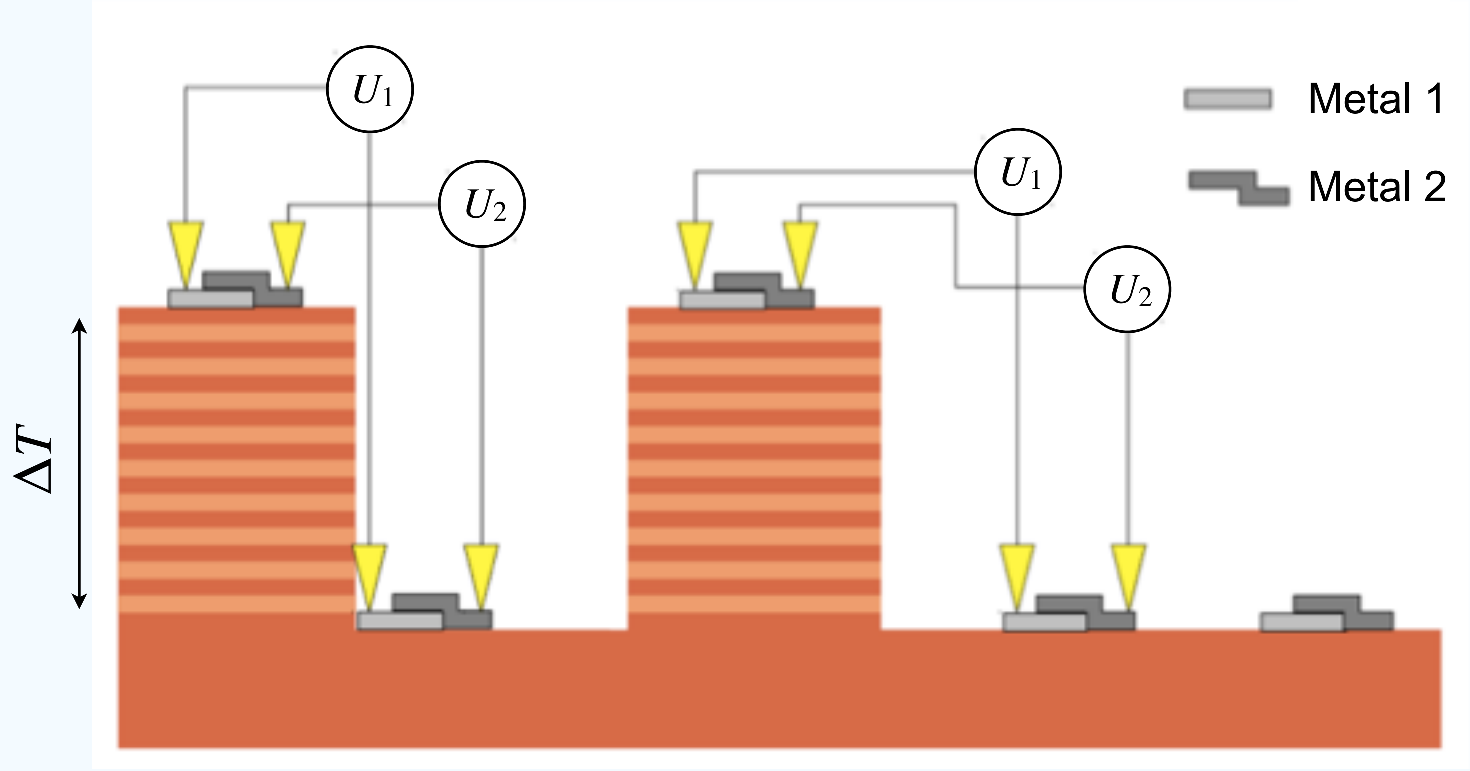

3ω measurements

- Deposition of a 100 nm insulating Al_2O_3 layer by ALD
- Reference sample without the multilayer structure
- Differential 3ω measurement of the thermal conductivity of thin films, $U_{3\omega} = \mathrm{f}(\kappa)$

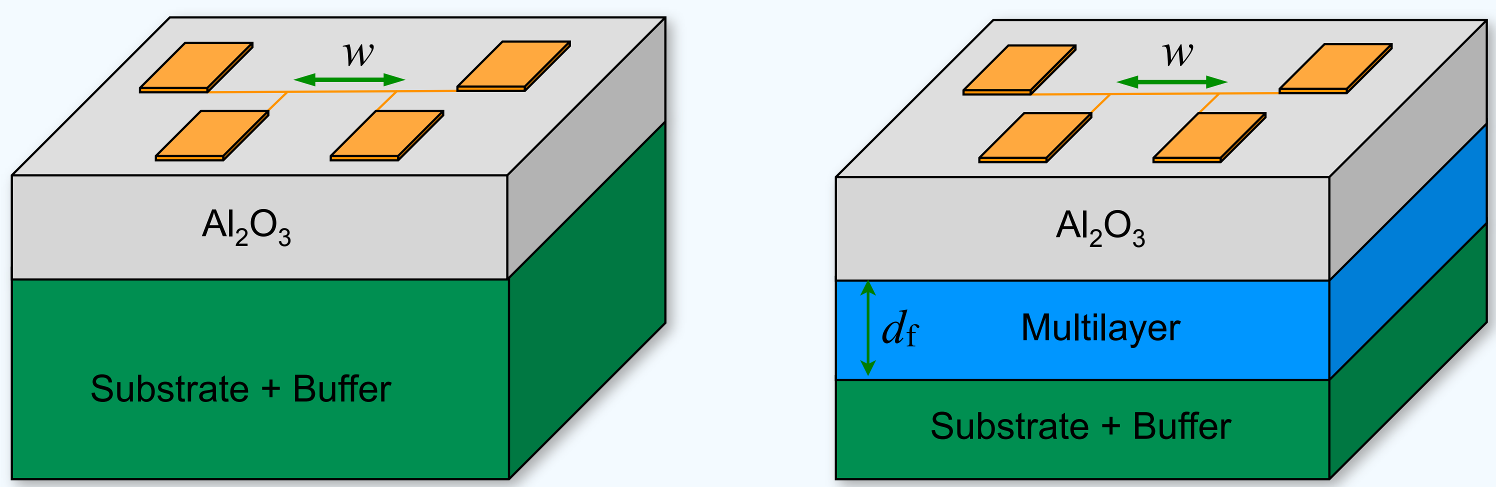

Temperature increase

- Current $I = I_0 \cos \omega t$ is related to the increase in temperature

  $\Delta T = \Delta T_0 \cos(2\omega t + \varphi)$

- Resistance of a metallic wire

  $R = R_0(1 + \alpha \Delta T)$

  Voltage $U = RI = R_0[1 + \alpha \Delta T_0 \cos(2\,\omega t + \varphi)]\, I_0 \cos \omega t$

- The $U_{3\omega} = 1/2\, I_0 R_0 \alpha \Delta T_0$ component contains information about the thermal properties of the underlying matter and is measured with a lock-in amplifier.

[Jacquot *et al*. ETC 1999]

Thermal conductivity of the thin film

$$\kappa = \frac{P(t_{\mathrm{tot}} - t_{\mathrm{ref}})}{2wb(\mathrm{Re}(\Delta T_{\mathrm{tot}}) - \mathrm{Re}(\Delta T_{\mathrm{ref}}))}$$

Measurement at a reference sample of the thickness t_{ref} and the sample containing the thin film with the total thickness t_{tot} (b width of the bolometer)

Thin film thermal conductivity

1D heat flow

Measurement with one bolometer stripe, width $b \gg d_f$

$\Delta T_f \rightarrow$ 1D thermal conductivity κ_{1D}

2D heat flow

Measurements with two bolometer stripes, b_1 and b_2

$\Delta T_f \rightarrow$ in-plane thermal conductivity $\kappa_{\|}$

$\rightarrow$ cross-plane thermal conductivity $\kappa_{\perp}$

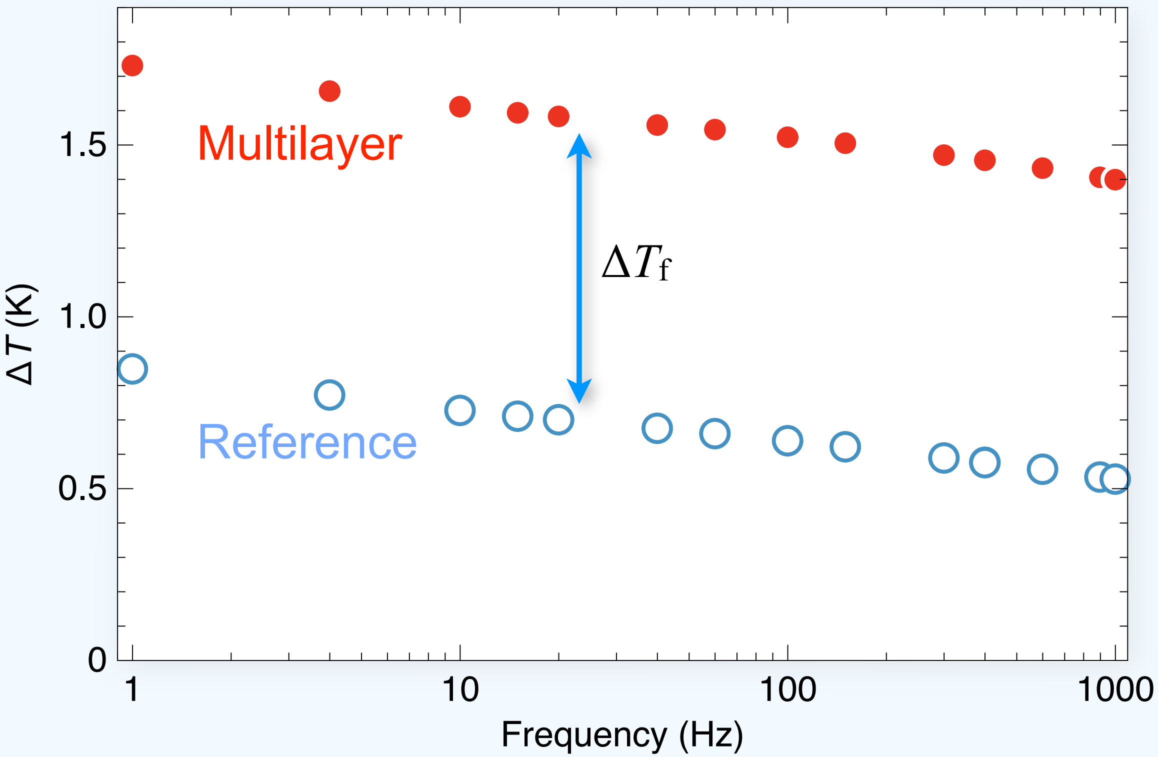

Bolometric temperature increase ΔT measured in a multilayer and a reference sample as a function of the frequency

SiGe Superlattices

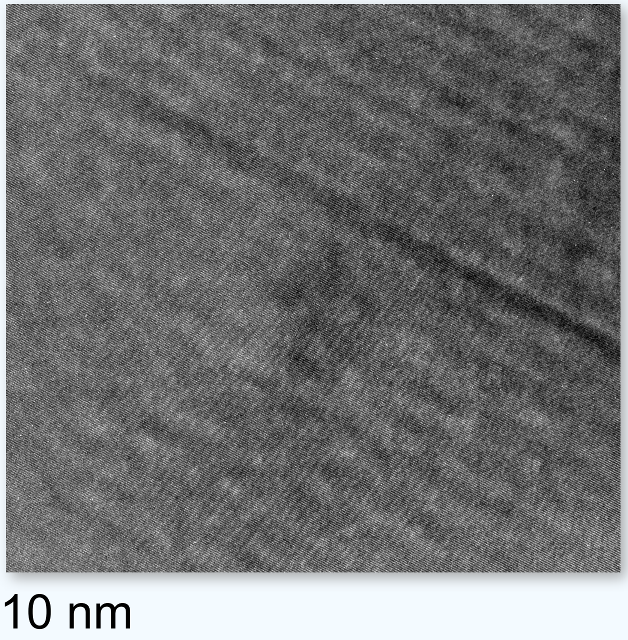

0.2 nm Ge + 3.3 nm Si
171×

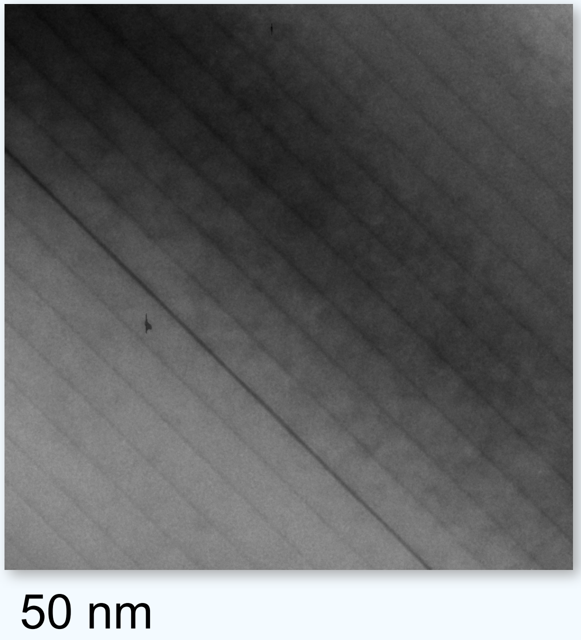

1.6 nm Ge + 12 nm Si
39×

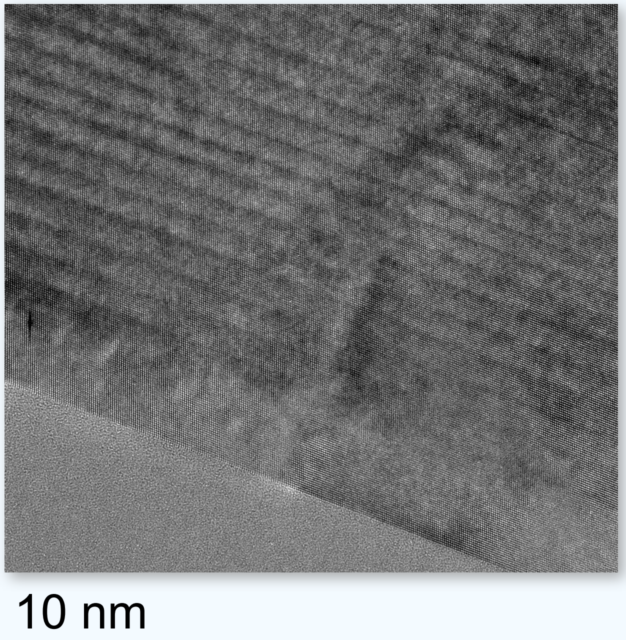

2 nm Ge + 1.5 nm Si
171×

total Ge content of the film

1.7 %	3.5 %	17 %

Thermal conductivity of periodic SL

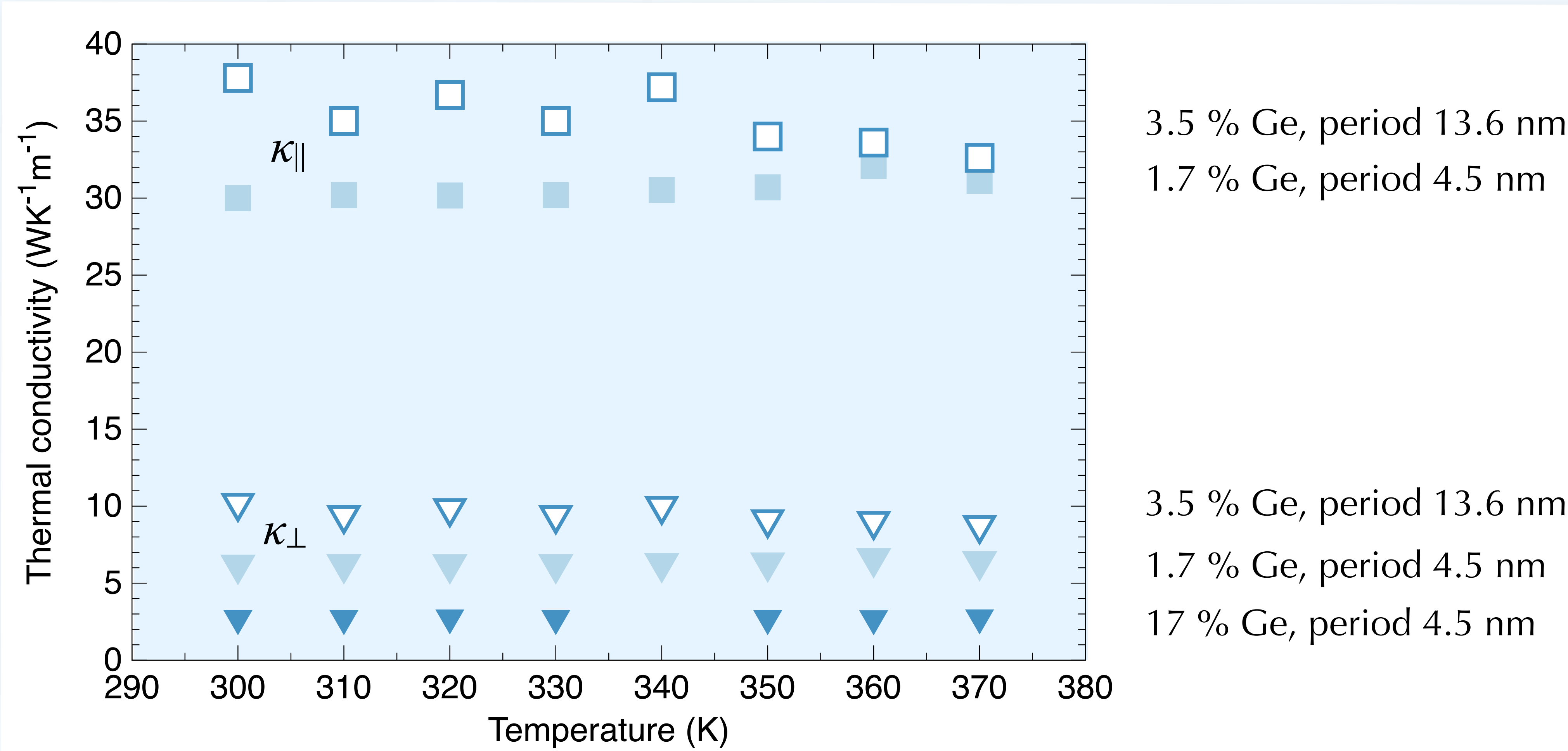

In-plane and cross-plane thermal conductivities for SLs with different Ge contents and periods

Aperiodic multilayers

20 nm

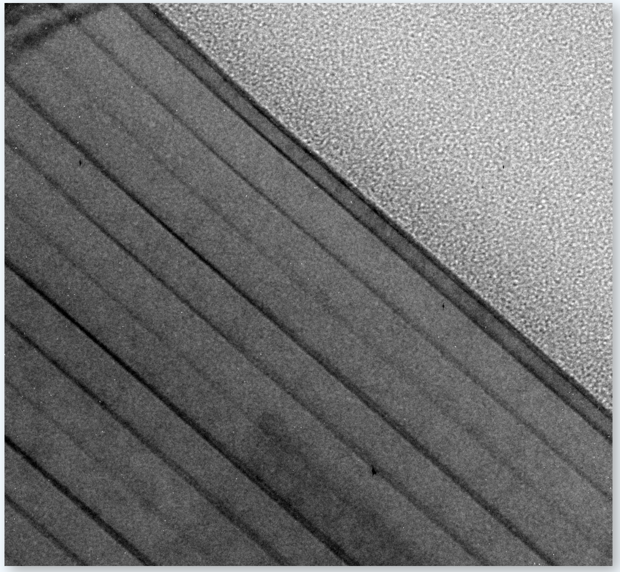

1.2 nm Ge + 12 nm Si
1.2 nm Ge + 12 nm Si
1.8 nm Ge + 12 nm Si
0.9 nm Ge + 12 nm Si
1.6 nm Ge + 12 nm Si
6×, ≈ 600 nm

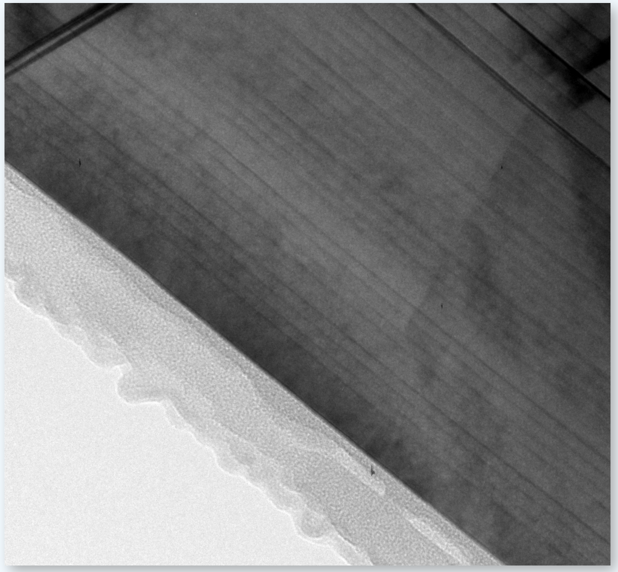

0.6 nm Ge + 4.1 nm Si
0.3 nm Ge + 5.1 nm Si
0.8 nm Ge + 4.8 nm Si
0.6 nm Ge + 5.7 nm Si
0.6 nm Ge + 3.8 nm Si
34×, ≈ 940 nm

Ge content

2.9 %	3.3 %

Results of random multilayers

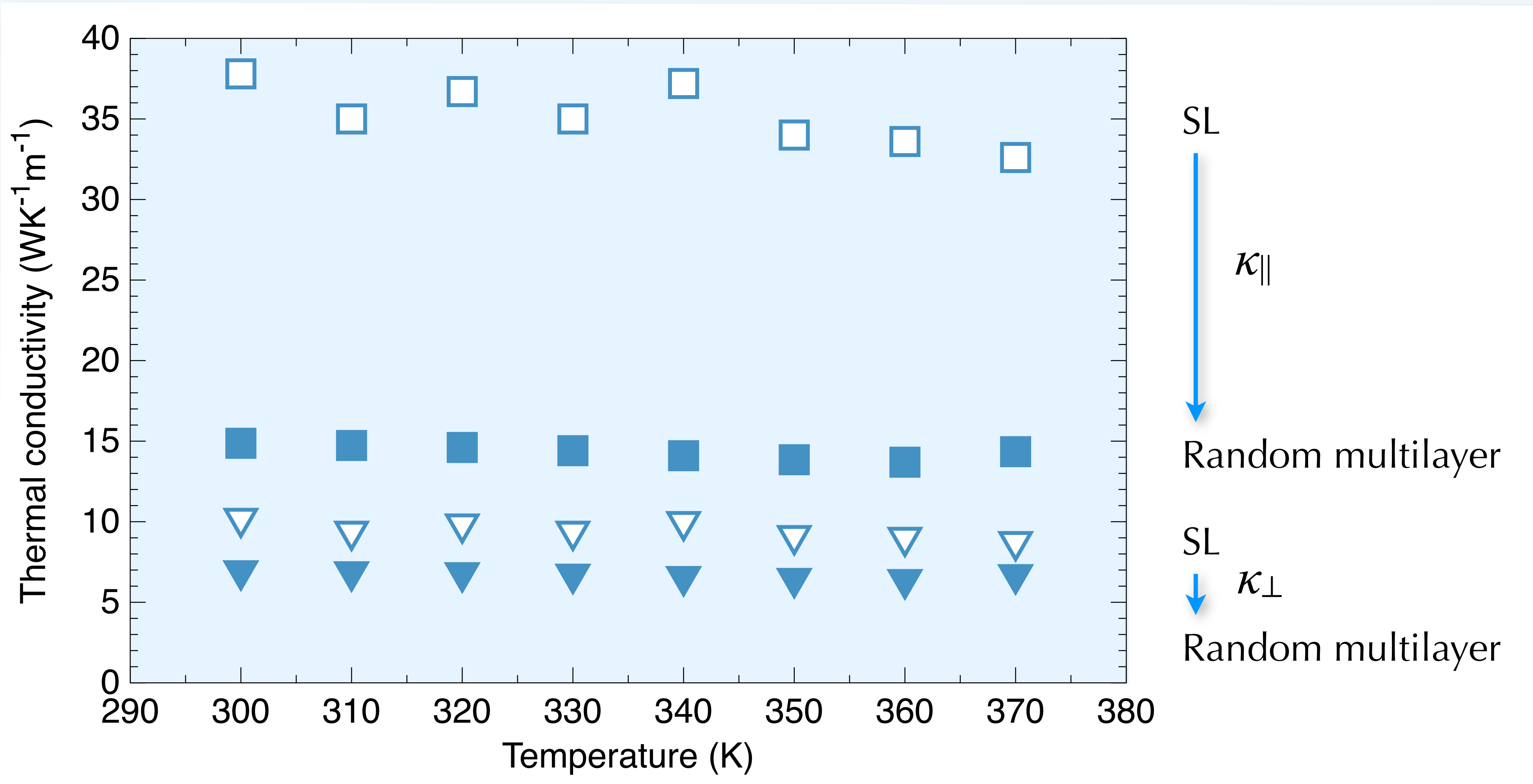

Thermal conductivities in a random multilayer (2.9 % Ge) in comparison to a superlattice(3.5 % Ge).

Defect issues

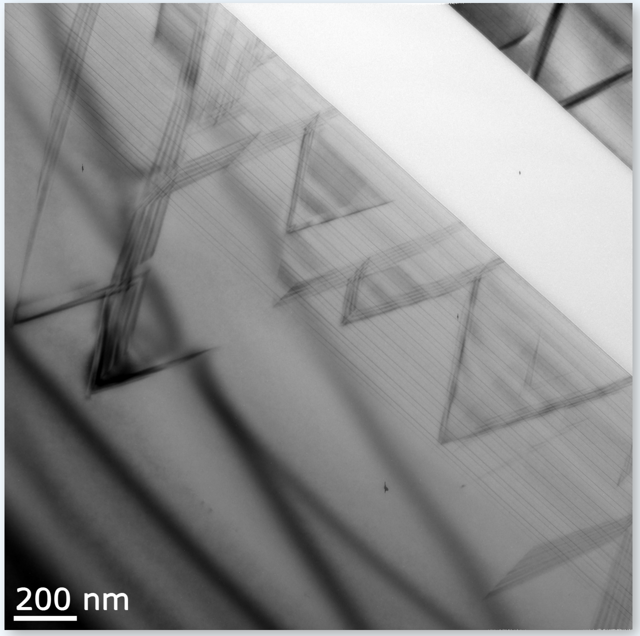

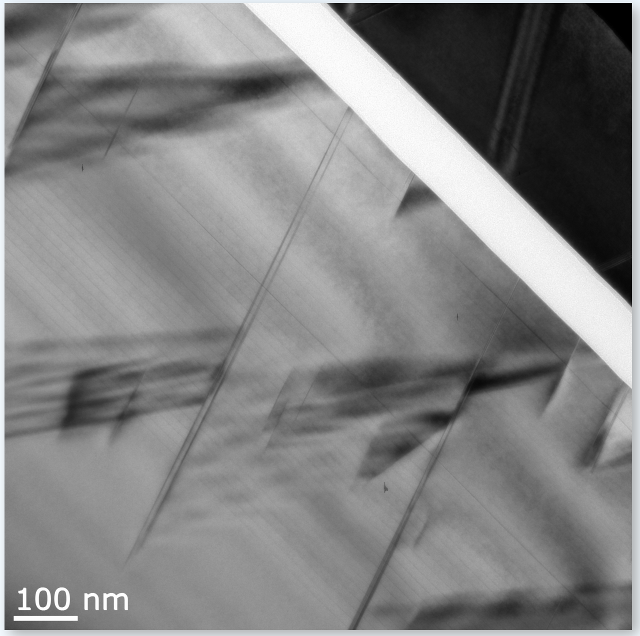

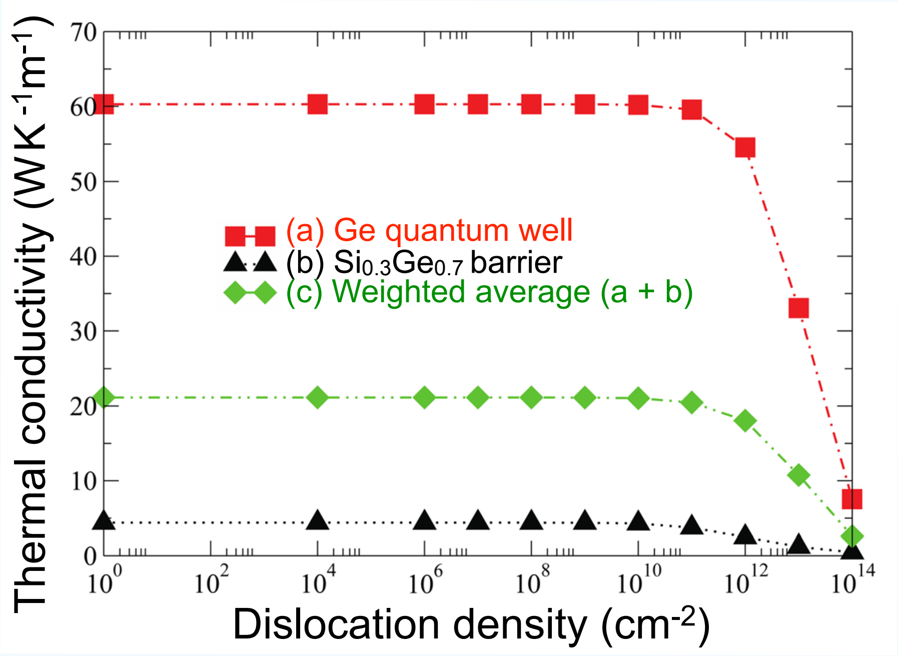

[Watling, Paul 2011]

Comparison of thermal conductivities

- Lowest $\kappa_\perp$ for SL with highest Ge content
- $\kappa_\perp$ a function of the SL period
  [cf. *e. g.* Rawat *et al*: J Appl Phys **105** (2009) 024909]
- Only a small reduction in $\kappa_\perp$ for random multilayers compared to SL observed due to low mass ratio in the multilayers investigated so far
- Random multilayers exhibit as well a decrease in $\kappa_\parallel$ by ≈ 50 %

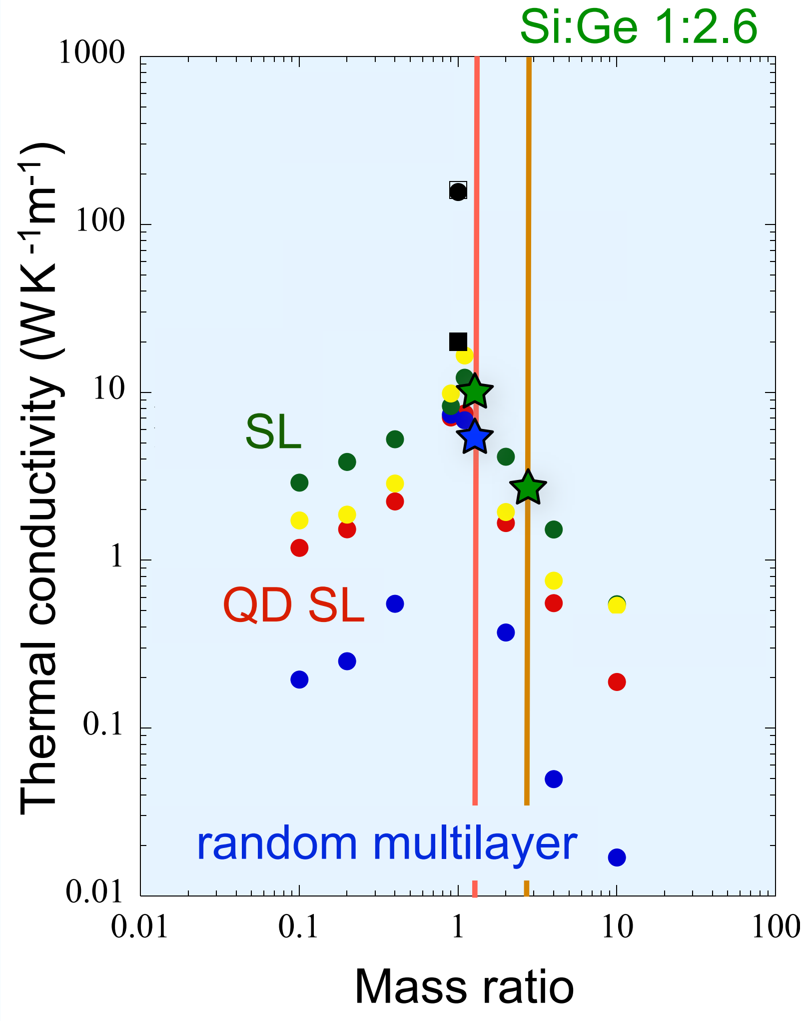

[Frachioni, White 2012]

Comparison of thermal conductivities

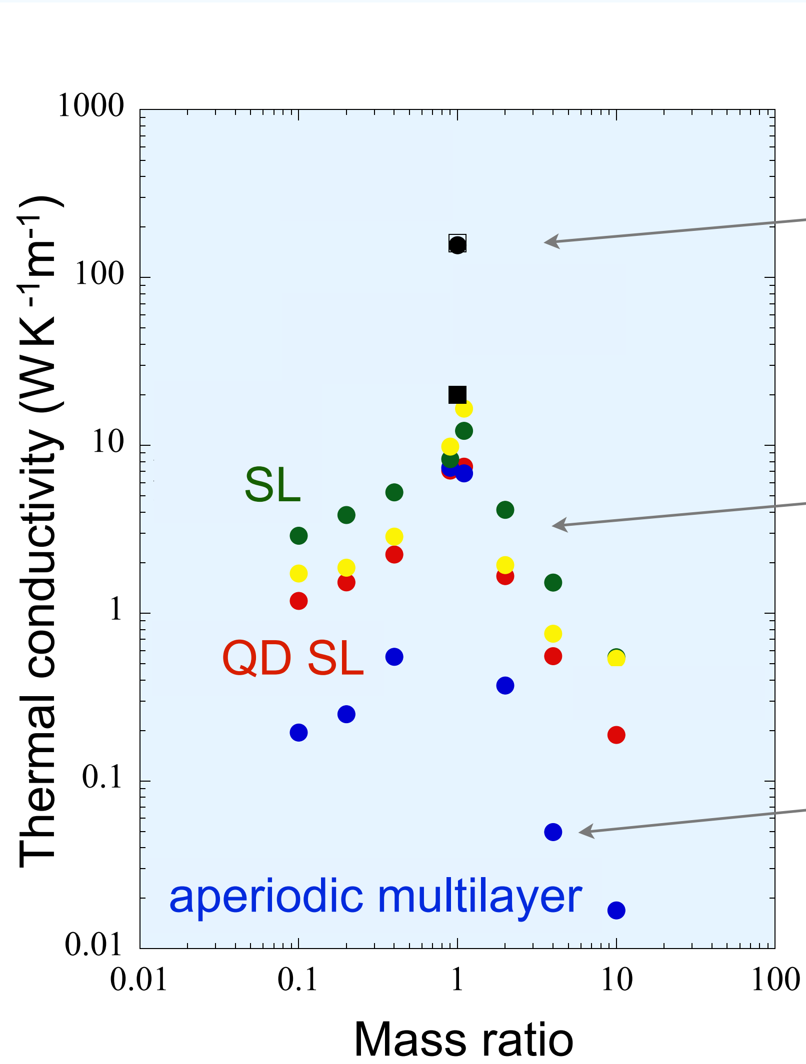

$\kappa(\mathrm{Si}) \approx 150\ \mathrm{W\,K^{-1}\,m^{-1}}$

$\kappa(\mathrm{SiGe\ SL}) \approx 2\ \mathrm{W\,K^{-1}\,m^{-1}}$

$m_{\mathrm{Ge}}/m_{\mathrm{Si}} \approx 2.6$

$\kappa(\mathrm{SiSn\ aML}) < 0.1\ \mathrm{W\,K^{-1}\,m^{-1}}$

$m_{\mathrm{Sn}}/m_{\mathrm{Si}} \approx 4.2$

Si–Ge–Sn

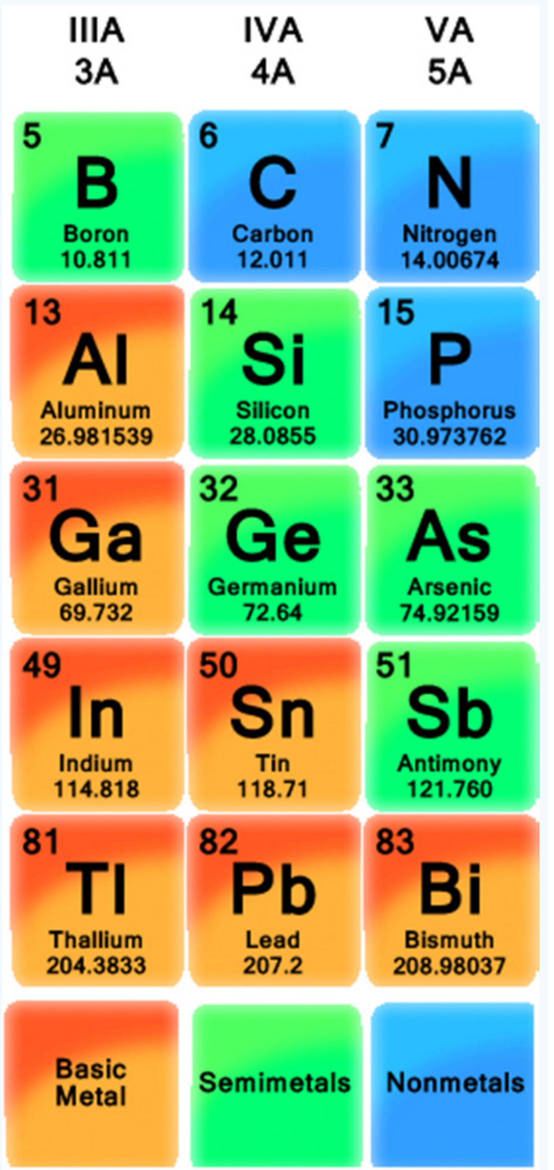
IIIA
3A
IVA
4A
VA
5A
5
B
Boron
10.811
6
C
Carbon
12.011
7
N
Nitrogen
14.00674
13
Al
Aluminum
26.981539
14
Si
Silicon
28.0855
15
P
Phosphorus
30.973762
31
Ga
Gallium
69.732
32
Ge
Germanium
72.64
33
As
Arsenic
74.92159
49
In
Indium
114.818
50
Sn
Tin
118.71
51
Sb
Antimony
121.760
81
Tl
Thallium
204.3833
82
Pb
Lead
207.2
83
Bi
Bismuth
208.98037
Basic Metal
Semimetals
Nonmetals

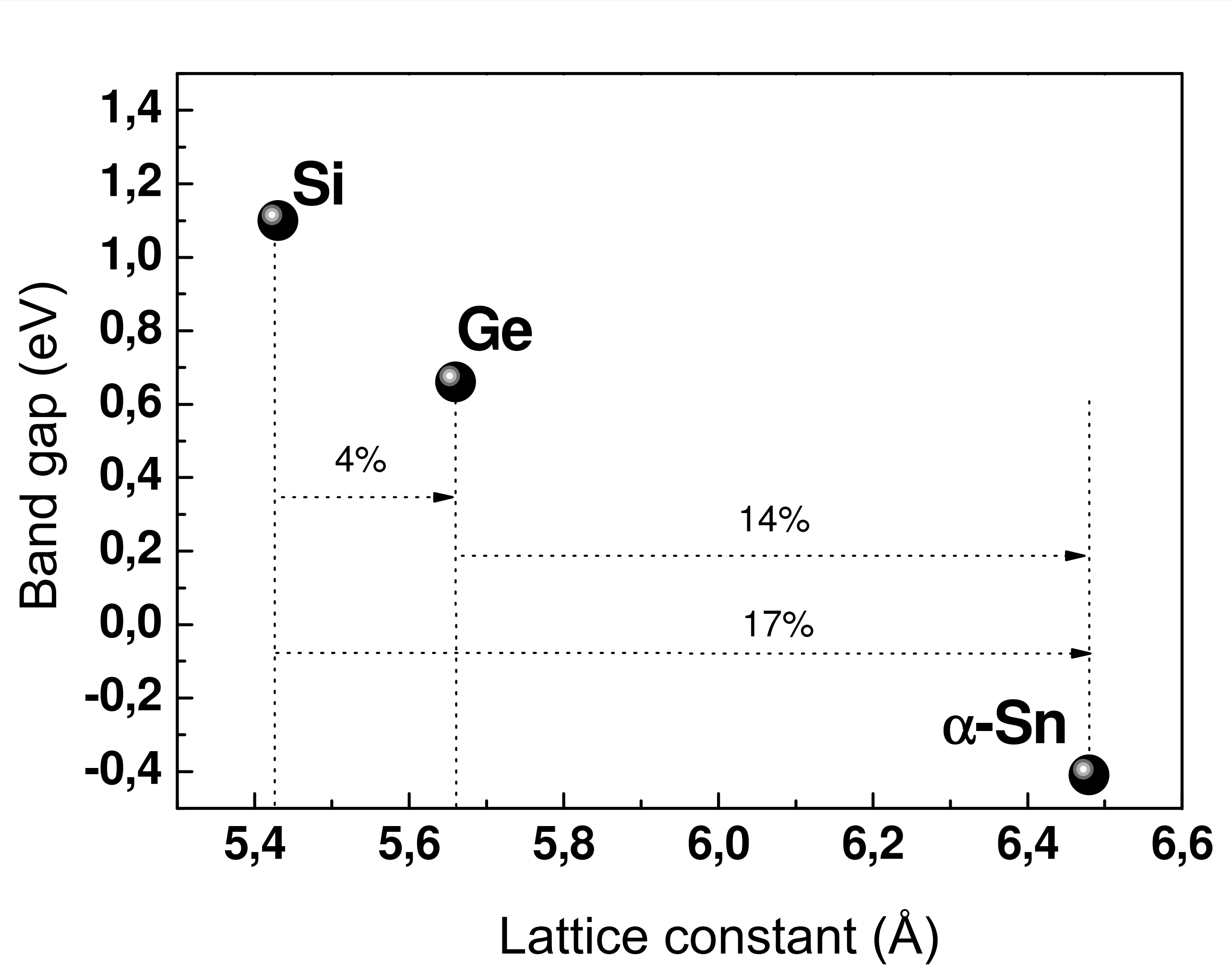
Band gap (eV)
1,4
1,2
1,0
0,8
0,6
0,4
0,2
0,0
-0,2
-0,4
Si
Ge
α-Sn
4%
14%
17%
5,4
5,6
5,8
6,0
6,2
6,4
6,6
Lattice constant (Å)

SiSn growth

MBE at 200 °C

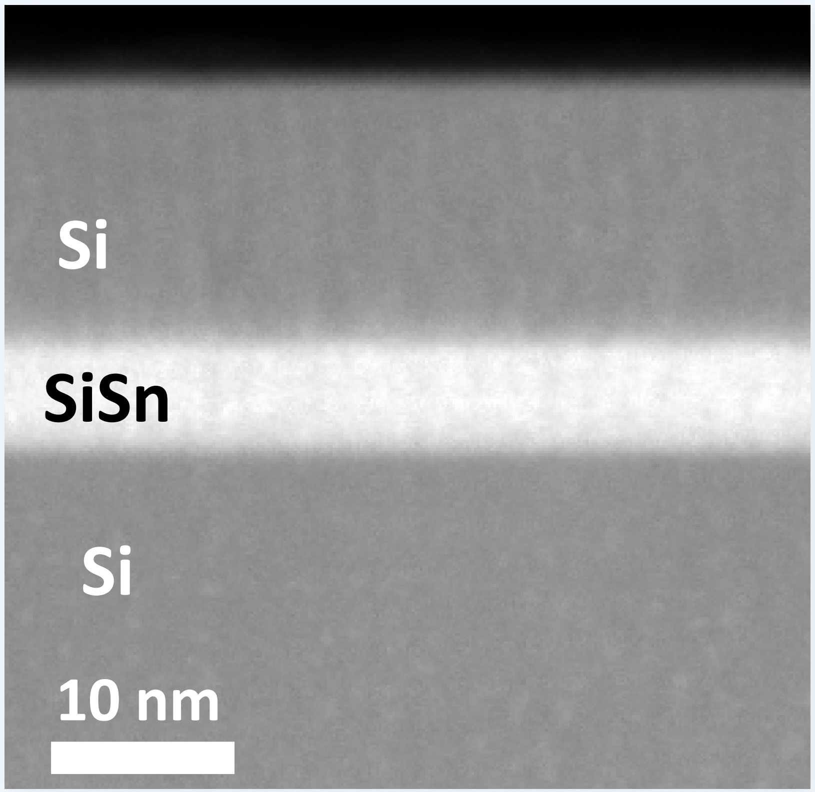

Cross-section TEM

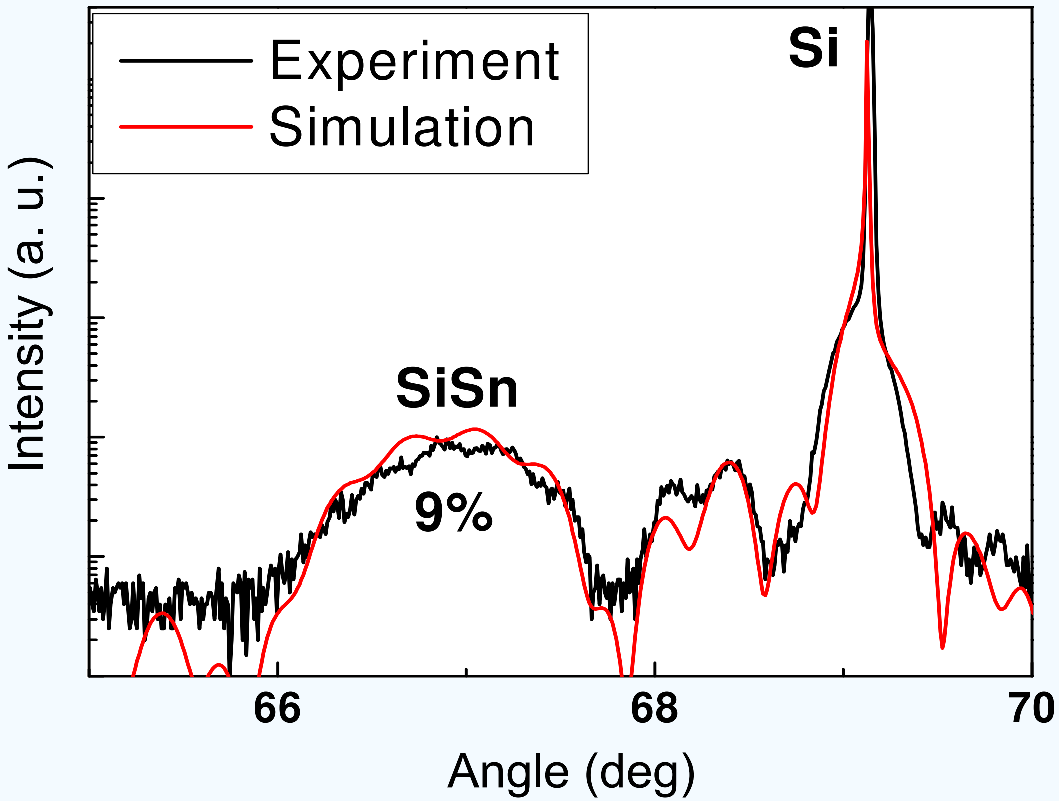

High-resolution X-ray Ω–2θ scan

Tonkikh *et al* J Cryst Growth **392** (2014) 49

SiSn multilayers

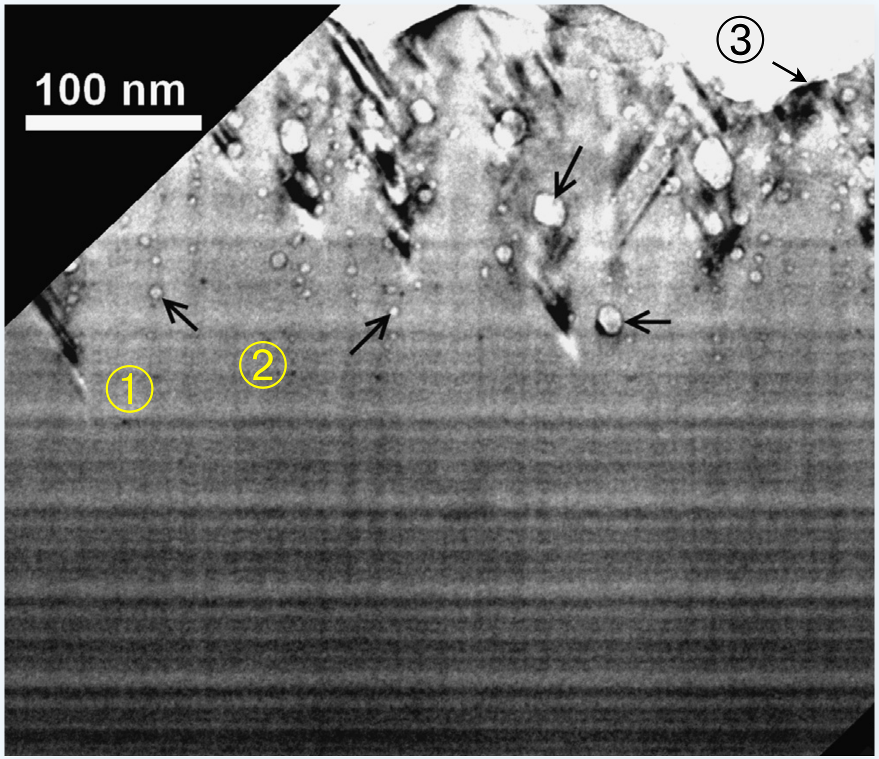

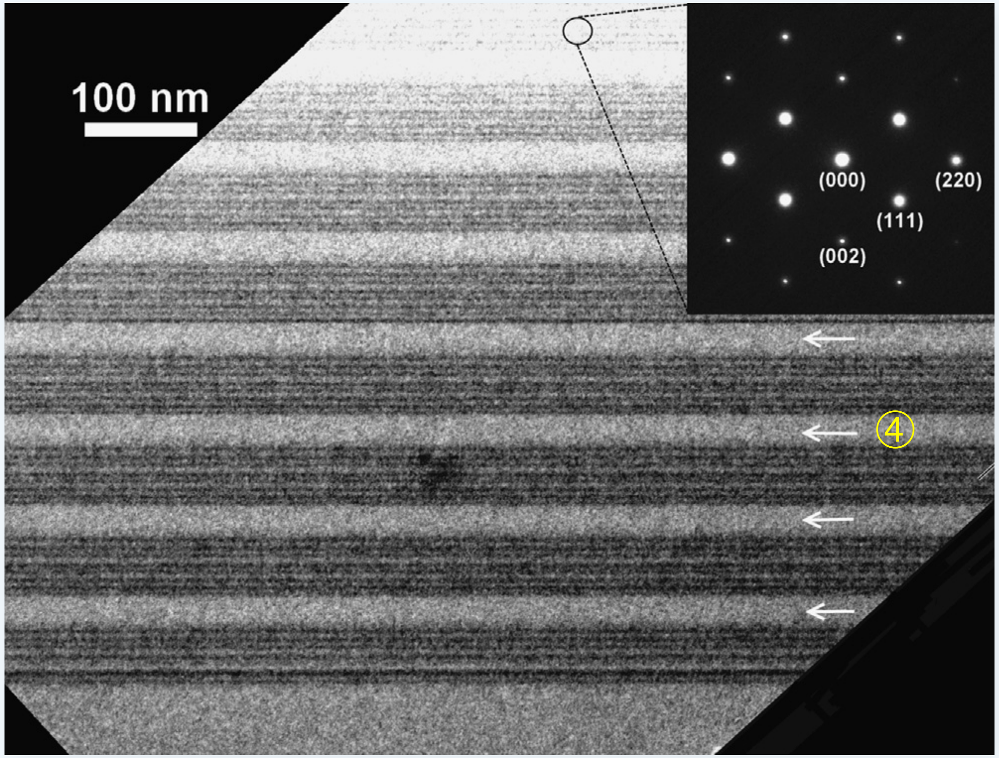

Defective growth with stacking faults ①, voids ②, amorphous Si/SiSn ③

Defect-free multilayers with Si insertions grown at high temperatures ④

Tonkikh *et al* J Cryst Growth **392** (2014) 49

Si–Ge nanowires

Geyer *et al* Nano Lett **9** (2009) 3106;
J Phys Chem **116** (2012) 13446

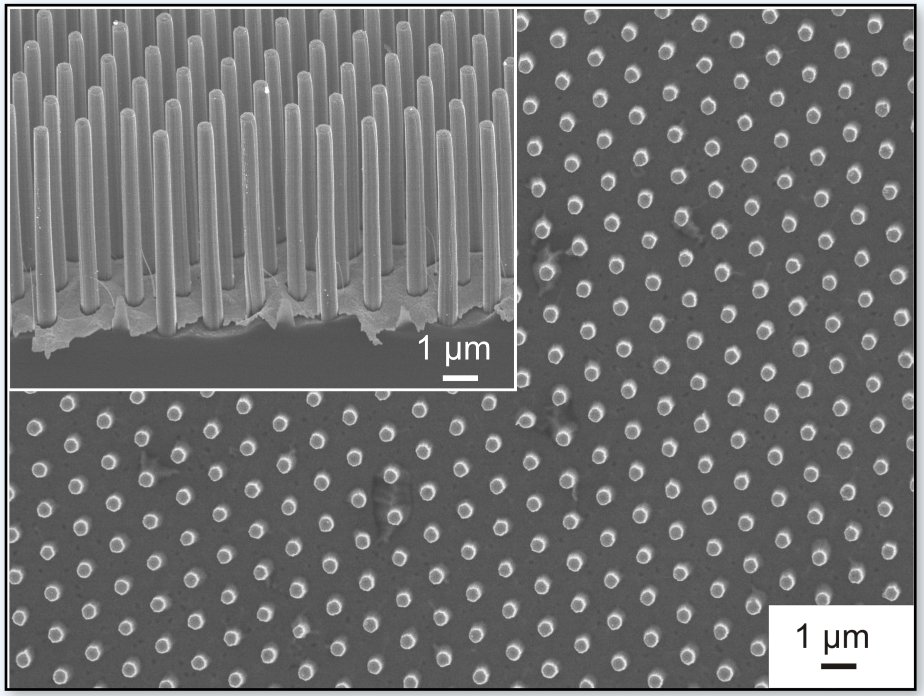

Silicon nanowires fabricated by metal-assisted etching

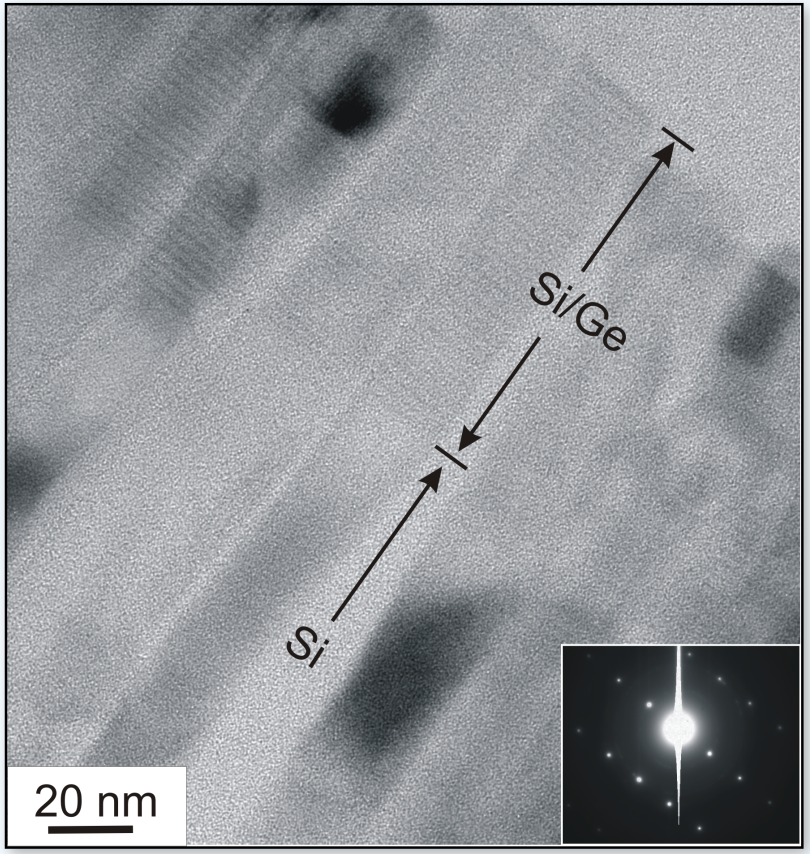

Si–Ge superlattice nanowires, ⌀ below 20 nm

➡ Further reduction of the thermal conductivity 100× smaller than bulk Si for ⌀ below 100 nm

Si nanoparticles in Al_2O_3

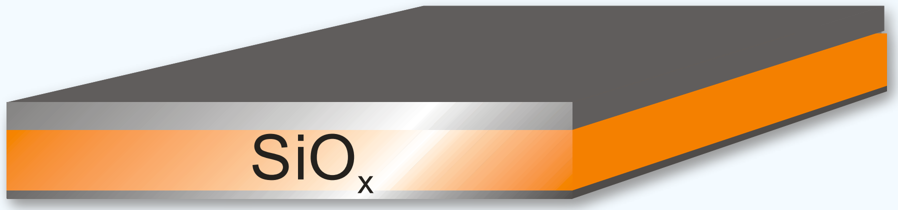

$$3\ SiO_2 + 4\ Al \rightarrow 3\ Si + 2\ Al_2O_3$$

Fabrication of nanoparticles in thin-film oxides

- Annealing $T > 560$ °C
- Conductivity ~ 100 S/cm, Seebeck coefficient $S \approx 400$ μV/K

Composite films with Si quantum dots

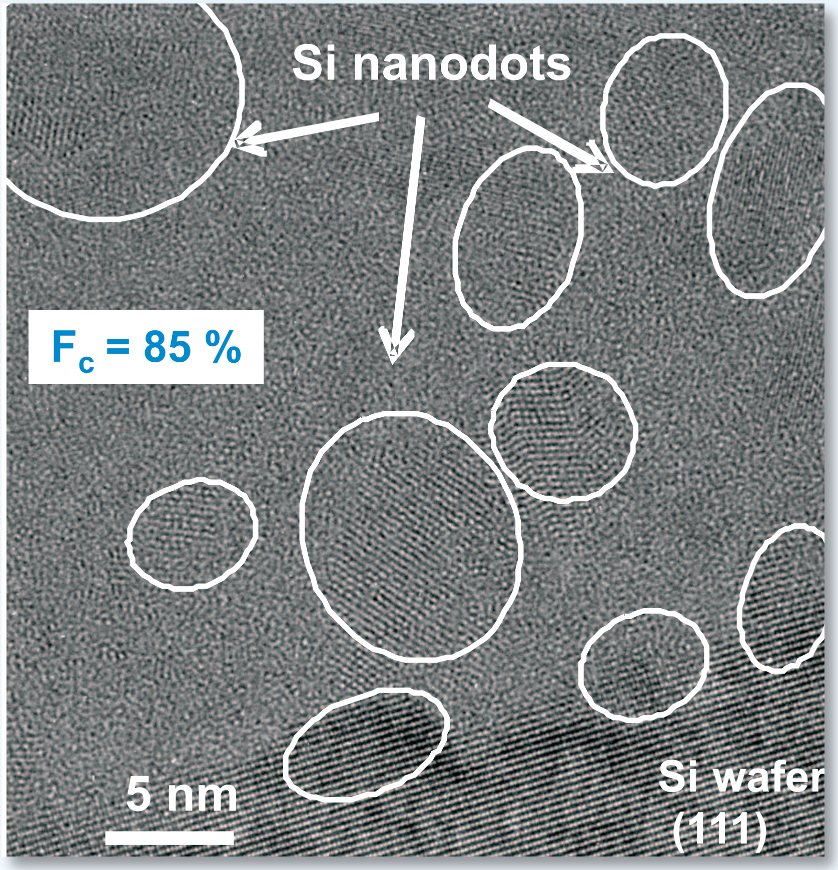

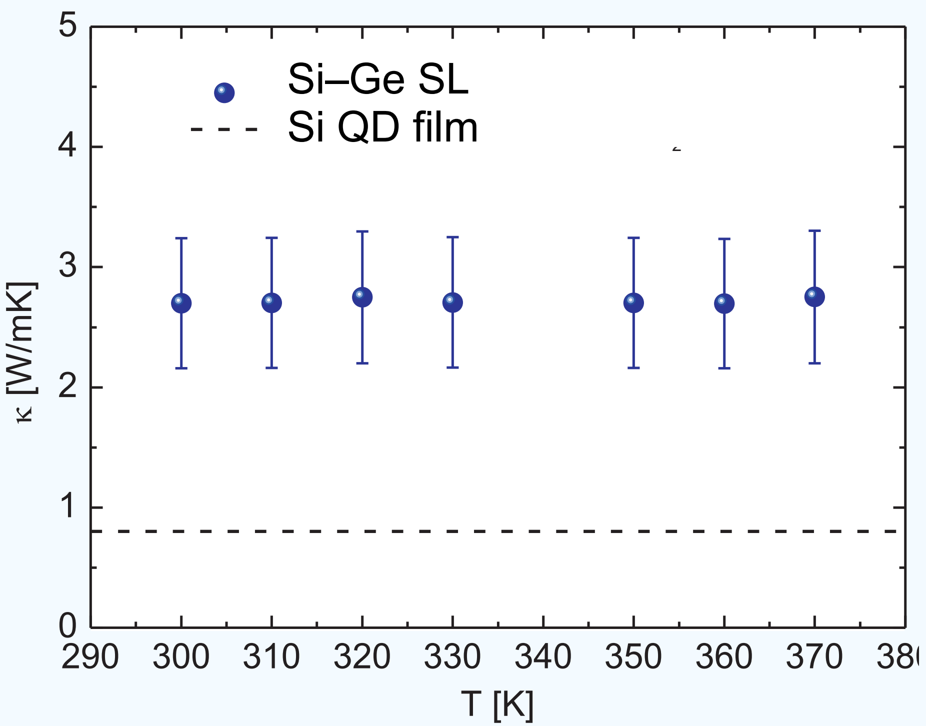

High power factor can be achieved near to the percolation limit ($\sigma > 100$ S/cm, $S \approx 400$ μV/K), thermal conductivity close to the oxide

Roczen *et al* J Non-Cryst Sol (2011) 10.1016/j.jnoncrysol.2011.11.024

Conclusions

- ➡ High-efficient thermoelectric thin-film devices based on Si and Ge possible
- ➡ Figure of merit for optimum structures higher than 2 for temperatures of RT … 300 °C
- ➡ Diverse approaches such as Si–Ge SL, incorporation of defects, fabrication of nanopillars
- ➡ Technological feasibility: Epitaxy, PVD *etc*.

References

- Snyder, Toberer: Nature Mater **7** (2008) 105.
- Fan, UC Santa Barbara, thesis 2002.
- Salleh, Ikeda: J Electron Mater **40** (2011) 903.
- Dismukes *et al*: J App Phys 35 (1964) 2899.
- Lee *et al*: Appl Phys Lett **70** (1997) 2957.
- Geballe, Hull: Phys. Rev **94** (1954) 1134.
- Frachioni, White: J Appl Phys **112** (2012) 14320.
- Hicks, Dresselhaus: Phys. Rev. B **47** (1993) 12727.
- Jacquot *et al*: ETS conference (1999).
- Tonkikh *et al* Thin Sol Films (2011) doi: 10.1016/j.tsf.2011.10.049.
- Tonkikh *et al* J Cryst Growth 392 (2014) 49
- Watling, Paul: J Appl Phys **110** (2011) 114508.
- Geyer *et al*: Nano Lett **9** (2009) 3106.
- Geyer *et al*: J Phys Chem **116** (2012) 13446.
- Roczen *et al* J Non-Cryst Sol (2011) 10.1016/j.jnoncrysol.2011.11.024.